ISSN 0036-0244, Russian Journal of Physical Chemistry A, 2014, Vol. 88, No. 12, pp. 2137–2145. © Pleiades Publishing, Ltd., 2014.

STRUCTURE OF MATTER AND QUANTUM CHEMISTRY

Investigations on Stabilities and Intermolecular Interactions of Different Naphthalene Derivatives Dimers by Using B3LYP and M06–2X Density Functional Calculations[1]

M. Karakaya[a,*], A. Çiçek[b], F. Ucun[b], and M. Yildiz[c]

[a] *Department of Energy Systems, Faculty of Engineering and Architecture, Sinop University, Sinop, 57000 Turkey*

[b] *Department of Physics, Faculty of Arts and Sciences, Süleyman Demirel University, Isparta, 32260 Turkey*

[c] *Department of Physics, Faculty of Sciences, Karamanoglu Mehmetbey University, Karaman, 70100 Turkey*

**e-mail: mkarakayafizik@hotmail.com*

Received April 19, 2014

Abstract—In this paper, the stabilities and hydrogen bond interactions of 4-chloro-1-naphthol, 1-hydroxynaphthalene and 1,4-dihydroxynaphthalene dimers have been theoretically investigated by means of study on binding energies with nonlocal hybrid three-parameter Lee–Yang–Parr, B3LYP, and M06-class functional calculations. Calculations on dimers aim to provide as a test of the efficacy of M06 calculations for intermolecular interaction calculations and more strongly bound systems. For hydroxyl- and halo-substituted derivatives of naphthalene, total electronic energies, their correction for the zero point vibrational energies with some calculated thermodynamic properties and their relative differences are together in order to discuss the rotamer structures. Static (hyper) polarizabilities and the electric dipole moments, frontier molecular orbital energy gaps and the relationships between them have been interpreted. Generally, they are seen that the calculated geometric parameters and spectral results were in a good agreement with the corresponding experimental data.

Keywords: naphthalene derivatives, density functional theory, M06-class functional method, vibration frequency

DOI: 10.1134/S0036024414120127

1. INTRODUCTION

Naphthalene, a white crystalline solid with a characteristic odor that is detectable at low concentrations [1], is classified as a polycyclic aromatic hydrocarbon and its structure can be considered as the fusion of couple benzene rings. Naphthalene derivatives have clinical potency that causes hemolysis with subsequent blockage of vomiting and headache [2, 3]. Also, they have various importances as intermediates for agricultural, pharmaceutical and industrial fields such as rubber, tanning and textile chemicals [4].

Many studies have been experimentally and theoretically reported in order to examine substituted hydroxyl derivatives of naphthalene by different methods in the recent past [5–8]. The mono-substituted hydroxyl derivatives of naphthalene are called as naphthol and give all the chemical reactions characteristic of phenols [9, 10]. The other hand, halo-substituted hydroxyaromatic compounds (among them the title compound) arc used as starting materials for the preparation of bis(hydroxyaromatic) compounds in chemical applications such as dyes, plastics, pharmaceuticals and pesticides, and in forming polymers [11].

Our aim of the present paper is to reveal the structures of 4-chloro-1-naphthol (CN), 1-hydroxynaphthalene (HN). 1,4-Dihydroxynaphthalene (DHN) by means of the spectral study and interaction energy by using density functional theory (DFT)–B3LYP level and M06-class functional calculations for dimer structures of these molecules. In addition, we aimed to compare theoretical results (IR and NMR chemical shifts) with the corresponding experimental data in this study.

2. COMPUTATIONAL DETAILS

Hydroxyl- and halo-substituted rotamers were optimized by density functional theory (DFT) [12] with nonlocal hybrid three-parameter Lee–Yang–Parr (B3LYP) [13, 14] level of theory with the 6-311G++(*d*,*p*) basis set in the Gaussian 03 [15] program. Vibrational frequencies of CN-a and CN-b were scaled with a scale factor of 0.9614 [16] by DFT–B3LYP method at 6-311++G(*d*,*p*) set. The assignments of the theoretical frequencies of CN were iden-

[1] The article is published in the original.

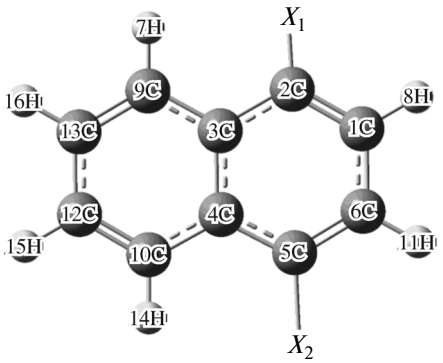

(a) X_1 = OH(17O, 18H), X_2 = C1(19Cl)
(b) X_1 = OH(17O, 18H), X_2 = H(19H)
(c) X_1 = OH(17O, 18H), X_2 = OH(19O, 20H)

Fig. 1. The view of molecular structures showing the atom numbering scheme for (a) 4-chloro-1-naphthol, (b) 1-hydroxynaphthalene, (c) 1,4-dihydroxynaphthalene.

tified by means of the potential energy distribution (PED) analysis using Vibrational Energy Distribution Analysis (VEDA 4) program [17] and these vibration modes were supported by using Gauss-View molecular visualization programs [18]. ^{1}H and ^{13}C NMR chemical shifts (in $CDCl_3$ and DMSO solvent) were done by Gauge Including Atomic Orbitals (GIAO) method [19, 20], and the solvent effects were taken into account by means of the PCM approximation [21]. In chemical shift calculations, tetramethylsilane (TMS) was used as a reference molecule. All the calculations for dimer structures were also performed at DFT method (B3LYP level) and M06–2X [22] theory with 6-31G(*d*,*p*) in Gaussian 09 [23] program. Basis set superposition error (BSSE) corrections and corrected binding energies were calculated by the counterpoise correction procedure (CP) [24].

3. RESULTS AND DISCUSSION

3.1. Rotameric Analysis and Geometric Parameters

Molecular structures showing the atom numbering scheme for CN, HN, and DHN are given Fig. 1. Primarily, in order to determine the substitution of hydroxyl group, potential energy surface (PES) scans are simply performed on 3C-2C-17O-18H torsion angles for CN and HN, θ_1[3C-2C-17O-18H] and θ_2[4C-5C-19O-20H] torsion angles (simultaneously) for DHN by B3LYP/6-31G(*d*) set level. The graphs of the PES scans of DHN compound are given Fig. 2 and θ_1, θ_2 are calculated as −180°. Sum of electronic and zero-point energies ($E_e + E_{ZPE}$) along with some calculated thermodynamic parameters (G and H) and their relative differences are reported for the considered rotamers of CN, HN, and DHN, all in gas phase, in Table 1. Relative differences of E_e are computed 1.56 (CN), 1.44 (HN), and 3.00 kcal/mol (DHN) can be interpreted as fairly moderate. Additionally, electric dipole moments, static dipole polarizabilities, first-order hyperpolarizabilities and energy gaps between the highest occupied molecular orbital (HOMO) and the lowest unoccupied molecular orbital (LUMO) for the rotamers of selected naphthalene derivatives are given in Table 2.

The averaged (isotropic) dipole polarizability is calculated using the following expressions defined as [25]:

$$\bar{\alpha} = \frac{\alpha_{xx} + \alpha_{yy} + \alpha_{zz}}{3}. \quad (1)$$

The overall in-plane and out-of-plane components of the polarizabilities are calculated as $1/2(\alpha_{xx} + \alpha_{yy})$ and

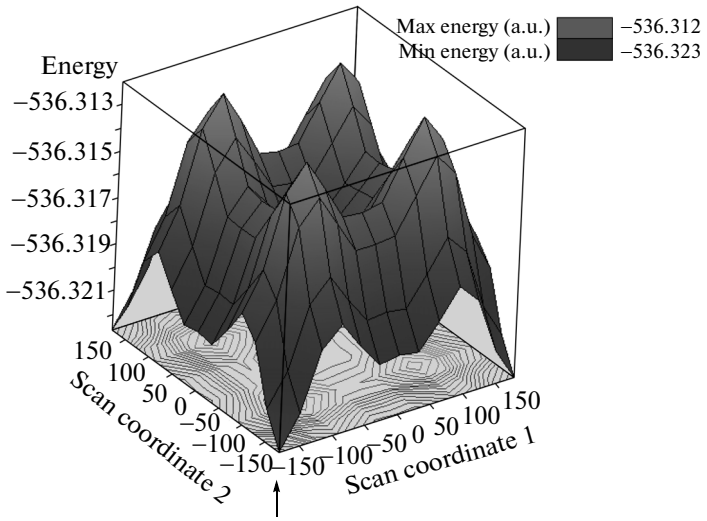

Fig. 2. Scan grid plot of 1,4-dihydroxynaphthalene for torsion angles 3C–2C–17O–18H and 4C–5C–19O–20H.

Table 1. Sum of electronic and zero-point energies ($E_e + E_{ZPE}$), thermodynamic parameters (G and H) and their relative differences for the rotamers of naphthalene derivatives in ab initio calculation

	CN-a	CN-b	HN-a	HN-b	DHN-a	DHN-b
E_e (hartree)	−920.857324	−920.854837	−461.236430	−461.234138	−536.481022	−536.476247
ΔE_e (kcal/mol)	0.00	1.561	0.00	1.438	0.00	2.996
$(E_e + E_{ZPE})$ (hartree)	−920.715847	−920.713485	−461.085552	−461.083349	−536.326406	−536.321526
$\Delta(E_e + E_{ZPE})$ (kcal/mol)	0.00	1.482	0.00	1.382	0.00	3.062
Thermodynamic parameters						
G (hartree)*	−920.750648	−920.748440	−461.118251	−461.116174	−536.360832	−536.355974
ΔG (kcal/mol)	0.00	1.386	0.00	1.303	0.00	3.048
H (hartree)*	−920.705540	−920.703100	−461.076482	−461.074220	−536.315826	−536.310979
ΔH (kcal/mol)	0.00	1.531	0.00	1.419	0.00	3.042

All results at B3LYP/6-311++G(d,p) basis set.|
* Sum of electronic and thermodynamic parameters values.

Table 2. The ab initio calculated electric dipole moments (Debye), static dipole polarizabilities, $\langle\alpha\rangle$ ($\times 10^{-24}$ esu), first-order hyperpolarizabilities, $\langle\beta\rangle$ ($\times 10^{-31}$ cm^5/esu) and homo-lumo energy gaps (a.u.) with their selected components for naphthalene derivatives

	CN-a	CN-b	HN-a	HN-b	DHN-a	DHN-b
μ_{tot}	1.8957	2.6136	1.3865	1.5769	2.5011	2.7321
α_{xx}	24.229	24.543	25.067	24.882	25.825	25.754
α_{yy}	25.423	25.134	19.651	19.837	20.864	21.088
α_{zz}	10.218	10.217	9.453	9.442	9.673	9.715
$\langle\alpha\rangle$	19.957	19.965	18.057	18.054	18.787	18.852
$\langle\beta\rangle$	9.39	19.52	20.37	24.48	13.86	31.84
$E_{HOMO}-E_{LUMO}$	0.1621	0.1576	0.1676	0.1632	0.1589	0.1489

All results at B3LYP/ 6-311++G(d,p) basis set.

α_{zz}, respectively [26]. Using the x, y, and z components of β the magnitude of the first hyper polarizabilities tensor can be calculated by:

$$\beta_{tot} = \sqrt{(\beta_x^2 + \beta_y^2 + \beta_z^2)}. \quad (2)$$

In summary, CN-a, HN-a, and DHN-a are more stable than the other rotamers in gas phase. As seen from Table 2, this can be attributed to an electrostatic viewpoint, taking into account the larger static electric dipole moment of the electronic ground state for CN-b, HN-b, and DHN-b rotamers [27]. It can be said that there is a contrasting relationship between the static first hyperpolarizabilities and HOMO–LUMO gaps [28]. HOMO–LUMO gaps have allowed the

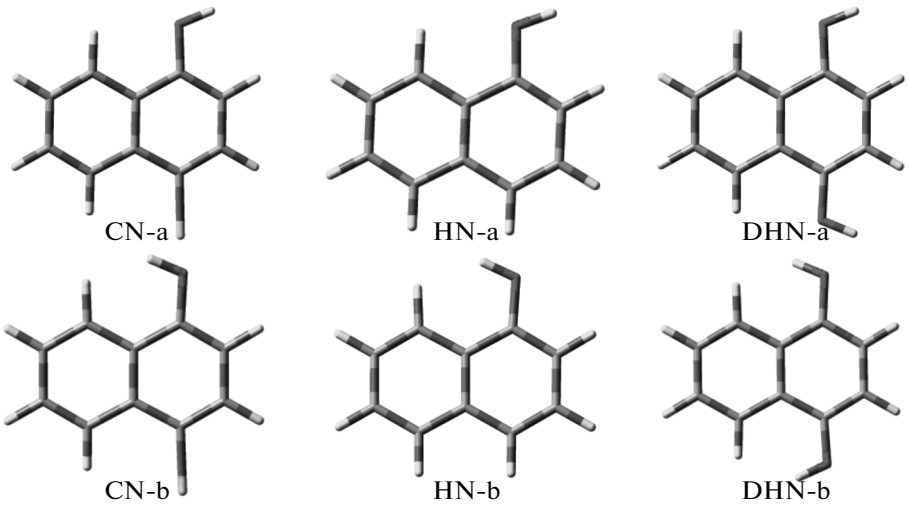

Fig. 3. The possible rotamers of CN, HN, DHN at DFT/B3LYP 6-311++G(d,p).

Table 3. Calculated geometric parameters for low-energy rotamers of CN, HN, DHN molecules

Parameters	Experimental	Calculated DFT/B3LYP method [6-311++G(*d*,*p*)] basis set		
bond lengths (Å)	CN [32]	CN-a	HN-a	DHN-a
Cl(19)–C(5)	1.748	1.764	–	–
O(17)–C(2)	1.394	1.367	1.369	1.374
C(1)–C(2)	1.355	1.375	1.377	1.373
C(2)–C(3)	1.415	1.426	1.426	1.426
C(1)–C(6)	1.410	1.411	1.413	1.415
C(5)–C(6)	1.356	1.370	1.373	1.373
C(4)–C(5)	1.417	1.424	1.421	1.426
C(4)–C(10)	1.413	1.418	1.420	1.417
C(3)–C(4)	1.431	1.433	1.430	1.429
C(10)–C(12)	1.367	1.375	1.375	1.376
C(12)–C(13)	1.401	1.412	1.414	1.412
C(9)–C(13)	1.364	1.375	1.375	1.376
C(3)–C(9)	1.417	1.417	1.418	1.417
O(17)–H(18)	–	0.963	0.963	0.963
C(1)–H(8)	–	1.085	1.086	1.086
C(9)–H(7)	–	1.082	1.082	1.082
C(6)–H(11)	–	1.082	1.084	1.086
C(10)–H(14)	–	1.082	1.085	1.082
C(12)–H(15)	–	1.084	1.084	1.084
C(13)–H(16)	–	1.084	1.084	1.084
		$R^2 = 0.9879$		
		Max. difference 0.027		
Bond angles (deg)				
C(2)–C(1)–C(6)	119.5	120.31	120.18	120.60
C(5)–C(6)–C(1)	120.5	120.31	120.76	120.60
C(6)–C(5)–C(4)	121.8	121.53	120.26	120.37
C(10)–C(4)–C(5)	124.0	123.72	122.08	121.96
C(10)–C(4)–C(3)	118.4	118.30	118.31	119.01
C(5)–C(4)–C(3)	117.6	117.97	119.61	119.03
C(12)–C(10)–C(4)	120.9	120.92	121.05	120.61
C(10)–C(12)–C(13)	120.6	120.61	120.33	120.38
C(9)–C(13)–C(12)	120.5	120.11	120.32	120.38
C(13)–C(9)–C(3)	120.6	120.67	120.46	120.61
C(2)–C(3)–C(9)	122.4	121.44	122.17	121.96
C(2)–C(3)–C(4)	118.6	119.18	118.28	119.03
C(9)–C(3)–C(4)	119.0	119.38	119.54	119.01
C(2)–O(17)–H(18)	–	109.70	109.55	109.48
C(4)–C(5)–Cl(19)	–	120.02	–	–
C(3)–C(9)–H(7)	–	118.55	118.82	118.63
C(2)–C(1)–H(8)	–	120.39	119.97	120.24
		$R^2 = 0.9468$		
		Max. difference 0.96		

molecular orbitals to overlap to have a proper electronic communication conjugation which is a marker of the intramolecular charge transfer from the electron donating group to the electron accepting group through the π-conjugation system [29, 30]. A similar result has been also indicated in a previous article published on a naphthalene-sulfonyl derivative [31]. Also, the non-linear optical response of an isolated molecule in an electric field can be represented as a Taylor series expansion of the total dipole moment. So, the higher values of calculated electric dipole moment can be associated with higher static polarizabilities.

The considered all rotamers obtained by optimizations at B3LYP/6-311++G(*d*,*p*) set are shown in Fig. 3. The calculated structure parameters for the

Table 4. Calculated vibrational frequencies for low-energy rotamer I and II of 4-chloro-1-naphthol

Mode no.	Sym-metry	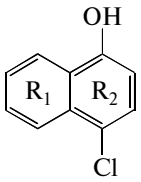 Assignments[a] (PED, %[b])	Experimental frequencies, cm^{-1} CN [33]		Calculated frequencies, cm^{-1} DFT/B3LYP 6-311++G(*d*,*p*)	
			IR	R	CN-a	CN-b
51	A'	$\nu_{OH}(100)$	3233br	–	3689	3703
50	A'	$(R_1 + R_2)[\nu_{CH}(98)$ sym]	3088sh	3089sh	3086	3085
49	A'	$(R_1 + R_2)[\nu_{CH}(93)$ asym]	3072sh	3074m	3084	3082
48	A'	$(R_1 + R_2)[\nu_{CH}(99)$ asym]	2955vs	–	3078	3069
47	A'	$R_1[\nu_{CH}(89)$ sym]	2927vs	3063sh	3061	3066
46	A'	$R_1[\nu_{CH}(95)$ asym]	2871sh	–	3047	3052
45	A'	$(R_1 + R_2)[\nu_{CH}(99)$ asym]	2855s	3017br	3038	3026
44	A'	$(R_1 + R_2)[\nu_{CC}(67)$ asym]	1601m	1603vw	1599	1602
43	A'	$(R_1 + R_2)[\nu_{CC}(62)$ asym]	1572w	1587sh	1572	1576
42	A'	$(R_1 + R_2)[\nu_{CC}(49)$ sym + $\delta_{CCC}(12)]$	1553br	1578s	1548	1546
41	A'	$(R_1 + R_2)[\nu_{CC}(24)$ asym] + $R_1[\delta_{HCC}(15)]$	1461m	1467m	1487	1488
40	A'	$(R_1 + R_2)[\nu_{CC}(24)$ asym + $\delta_{HCC}(39)]$	1448m	1444sh	1435	1426
39	A'	$(R_1 + R_2)[\delta_{HCC}(46)]$	1403w	1435m	1409	1409
38	A'	$(R_1 + R_2)[\delta_{HCC}(39)]$	1377s	1376vs	1364	1358
37	A'	$(R_1 + R_2)[\nu_{CC}(50)$ asym]	1348s	1349vw	1339	1342
36	A'	$(R_1 + R_2)[\nu_{CC}(60)$ asym]	1316w	–	1314	1318
35	A'	$(R_1 + R_2)[\delta_{HCC}(27) + \nu_{CC}(16)$ asym] + $\nu_{OC}(16)$	1261s	1266vw	1243	1247
34	A'	$(R_1 + R_2)[\delta_{HCC}(41) + \nu_{CC}(15)$ asym] + $\nu_{OC}(14)$	1240s	1203vw	1218	1223
33	A'	$\delta_{HOC}(31) + (R_1+R_2)[\delta_{HCC}(11)]$	1201s	1162w	1180	1175
32	A'	$R_1[\delta_{HCC}(24)] + \delta_{HOC}(17) + R_2[\nu_{CC}(12)]$	1166vw	–	1171	1155
31	A'	$(R_1 + R_2)[\delta_{HCC}(51)]$	1159m	1155sh	1136	1142
30	A'	$(R_1 + R_2)[\nu_{CC}(20)$ asym] + $R_1[\delta_{HCC}(17)]$ + $\delta_{HOC}(14)$	1124w	1126w	1122	1132
29	A'	$(R_1 + R_2)[\delta_{HCC}(22) + \nu_{CC}(15)$ asym]	1055s	1058vw	1099	1100
28	A'	$(R_1 + R_2)[\delta_{CCC}(23)] + \nu_{OC}(14)$	1043sh	1026m	1025	1027
27	A'	$(R_1 + R_2)[\nu_{CC}(60)$ asym]	1026m	–	1006	1007
26	A''	$(R_1 + R_2)[\tau_{CCC}(74)]$	979vw	–	965	961
25	A''	$(R_1 + R_2)[\tau_{CCC}(84)]$	951w	944w	944	923
24	A'	$(R_1 + R_2)[\delta_{CCC}(42)] + \nu_{OC}(17)$	945w	906vw	912	909
23	A''	$(R_1 + R_2)[\tau_{CCC}(74)]$	860vw	–	880	907
22	A''	$(R_1 + R_2)[\tau_{CCC}(85)]$	811s	810vw	842	825
21	A''	$(R_1 + R_2)[\tau_{CCC}(73)] + R_2[\gamma_{OCCC}(16)]$	771sh	793vw	779	809
20	A'	$(R_1 + R_2)[\delta_{CCC}(56)]$	764m	769vw	772	771
19	A''	$(R_1 + R_2)[\tau_{CCC}(52)] + R_1[\tau_{CCCC}(12)]$	751s	–	751	744
18	A''	$(R_1 + R_2)[\tau_{CCCC}(37) + \tau_{CCC}(22)$ + $\gamma_{CCCC}(14)]$	717w	722s	741	730
17	A'	$(R_1 + R_2)[\delta_{CCC}(41) + \nu_{CC}(13)$ sym] + $\nu_{OC}(11)$	652m	–	699	700
16	A'	$(R_1 + R_2)[\delta_{CCC}(37)] + \nu_{ClC}(25)$	629w	652m	631	630

Table 4. (Contd.)

Mode no.	Sym-metry	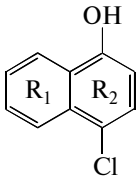 Assignments[a] (PED, %[b])	Experimental frequencies, cm^{-1} CN [33]		Calculated frequencies, cm^{-1} DFT/B3LYP 6-311++G(*d*,*p*)	
			IR	R	CN-a	CN-b
15	A''	$(R_1 + R_2)[\tau_{CCCC}(49)] + \gamma_{OCCC}(14)$	584w	–	615	616
14	A''	$\gamma_{CCCC}(17) + \gamma_{OCCC}(12) + \gamma_{ClCCC}(10) + (R_1 + R_2)[\tau_{CCCC}(14)]$	559vw	556w	575	570
13	A'	$(R_1 + R_2)[\delta_{CCC}(31)] + \delta_{OCC}(25)$	525w	527m	531	530
12	A′	$\delta_{OCC}(15) + \delta_{ClCC}(15) + R_2[\nu_{CC}(10)]$	–	–	510	508
11	A'	$(R_1 + R_2)[\delta_{CCC}(40)]$	480m	482m	468	464
10	A''	$(R_1 + R_2)[\tau_{CCCC}(83)] + R_1[\tau_{HCCC}(12)]$	458vw	463vw	453	456
09	A''	$R_1[\tau_{CCCC}(57)] + \gamma_{OCCC}(11)$	–	418vw	411	408
08	A'	$\nu_{ClC}(40) + (R_1 + R_2)[\delta_{CCC}(25)]$	–	381m	358	359
07	A''	$\gamma_{ClCCC}(39) + (R_1 + R_2)[\tau_{CCCC}(21)] + \gamma_{OCCC}(20)$	–	359vw	335	333
06	A'	$\delta_{OCC}(37) + \delta_{CCC}(21) + \delta_{ClCC}(13)]$	–	–	288	300
05	A''	$\tau_{HOCC}(90)$	–	–	275	235
04	A'	$\delta_{ClCC}(56) + \delta_{CCC}(25)$	–	227s	209	211
03	A''	$\gamma_{CCCC}(48) + R_1[_{CCCC}(21)] + \gamma_{ClCCC}(10)$	–	165m	178	177
02	A''	$(R_1 + R_2)[\tau_{CCCC}(84)]$	–	136m	130	115
01	A''	$(R_1 + R_2)[\tau_{CCCC}(55)] + \gamma_{ClCCC}(29)$	–	107vw	103	102
				$R^2 =$	0.9948	0.9944
				RMSD =	70.7623	72.8324

[a] Vibrational modes assignments for CN-a.
[b] Potential energy distribution (PED), less than 10% are not shown.
ν, stretching; δ, bending; γ, out of plane bending; τ, torsion modes; sym, symmetric; asym, anti symmetric; w, weak; m, medium; s, strong; v, very; sh, shoulder; br, broad.

low-energy rotamers of CN, HN, DHN molecules are summarized in Table 3, in accordance with the atom numberings in Fig. 2. Table 3 also compares the calculated bond lengths and angles with published experimental X-ray crystallographic data of CN [32]. The Correlation coefficients (R^2) shows that the theoretical results were found to comply with the corresponding experimental data, highly.

3.2. Spectral Analysis

The resulting vibration frequencies for the forms of CN are given in Tables 4. For comparison, the experimental vibration frequencies (Infrared and Raman) of the compounds are also given in the tables [33]. As realized from Fig. 3, CN-a molecule is planar and belongs to the Cs point group. So, the vibrations being symmetric through the mirror plane σ_h will belong to the species 35*A*', the ones being anti-symmetric to the species 16*A*'' and total numbers of vibration modes are 51. Assignments of all the fundamental vibration modes obtained by PED analysis and the symmetry species of ail the vibration modes also written in Tables 4. For C–H (aromatic) stretching, the frequencies values are computed at the ranges of 3038–3086 cm^{-1} for CN-a and 3026–3085 cm^{-1} for CN-b, with the highest percentile (% PED). Also, C=C stretching mode are calculated as 1435–1599 and 1426–1602 cm^{-1}, for CN-a and CN-b, respectively. The absorption of the O–H stretching vibration is observed at 3291 cm^{-1}, the strong and broad peak, in the spectrum of 1,5-dihydroxynaphthalene and the bands at 1598, 1524 cm^{-1} are ascribed to C=C stretching, 1257 cm^{-1} to C–OH stretching vibrations by Lu et al. [34]. Correlations values (R^2) and mean root-mean-square deviation (RMSD) between the experimental and calculated frequencies can be seen in the last lines of Tables 4. Statistical results show that the agreements with experimental data were better level for CN-a form than their other one. Besides, calculated ^1H and ^{13}C NMR chemical shifts (with respect to TMS) for all the forms of the title compounds are tabulated in Table 5. The experimental values of CN-a (in $CDCl_3$), HN-a (in $CDCl_3$), and DHN-a (DMSO-d_6) have been obtained from Spectral Database for Organic Compounds Web Page [35]. Consequently, the correlation factors between the experimental and theoreti-

Table 5. Experimental and calculated chemical shift values (with respect to TMS) for low-energy rotamers of CN, HN, DHN molecules at B3LYP/6-311++G(*d*,*p*) basis set with GIAO method

Atoms	CN-a (in $CDCl_3$) Shielding, ppm		HN-a (in $CDCl_3$) Shielding, ppm		DHN-a (in DMSO-d_6) Shielding, ppm	
	experimental*, ppm	calculated	experimental*, ppm	calculated	experimental*, ppm	calculated
C1	108.60	111.784	108.88	111.657	107.92	111.836
C2	150.46	160.274	151.16	161.325	145.43	154.067
C3	125.39	131.672	124.41	129.264	125.33	129.805
C4	131.54	138.408	134.77	140.473	125.33	129.805
C5	123.54	136.655	120.82	125.716	145.43	154.067
C6	125.72	132.614	125.84	132.219	107.92	111.836
C9	122.07	129.846	121.44	129.204	121.88	127.463
C10	124.45	129.812	127.71	134.150	121.88	127.463
C12	126.02	134.452	126.43	132.590	124.66	132.151
C13	127.56	131.644	125.33	130.956	124.66	132.151
R^2		0.9520		0.9926		0.9947
H7	8.36	8.783	8.161	8.839	8.076	8.727
H8	6.692	7.057	6.734	7.089	6.703	7.110
H11	7.351	7.756	7.259	7.636	6.703	7.110
H14	8.36	8.439	7.786	8.395	8.076	8.727
H15	7.53	8.095	7.45	7.884	7.431	8.127
H16	7.61	8.005	7.47	7.960	7.431	8.127
H17	–	–	–	–	–	–
H18	5.31	5.673	5.43	5.738	9.326	5.828
H19	–	–	7.417	7.832	–	–
H20	–	–	–	–	9.326	5.828
R^2		0.9811		0.9936		0.2223

* Ref. [35].

Table 6. Counterpoise (CP) corrected energy, basis set superposition error (BSSE), binding energy (ΔE), and calculated by using DFT and M06 calculations for naphthalene derivatives dimers

	CP energy, hartree		CP BSSE energy, kcal/mol		ΔE*, kcal/mol	
	B3LYP	M06/2X	B3LYP	M06/2X	B3LYP	M06/2X
CN-a	−1841.44295	−1841.00219	2.899	2.430	−3.989 (−6.888)	−6.754 (−9.184)
HN-a	−922.25760	−921.86553	3.020	2.509	−4.085 (−7.105)	−6.791 (−9.300)
DHN-a	−1072.69309	−1072.25701	3.188	2.492	−4.199 (−7.387)	−7.017 (−9.509)

All values at 6-31G(*d*,*p*) basis set.
* BSSE-corrected (uncorrected) values.

cal chemical shifts can be also seen in the last lines of the Table 5. According to these values it can be staled that the agreement between the experimental and calculated chemical shifts is good.

3.3. Dimer Structures

Firstly, the geometries of CN-a, HN-a, and DHN-a dimers are obtained by DFT–B3LYP functional and M06/2X calculations with 6-31G(*d*,*p*). All computed binding energy and CP–BSSE energy of the dimers have been summarized by the counterpoise correction procedure in Table 6. As shown in Fig. 4, the most stable dimer structures obtained by B3LYP functional theory have linear and single strong O–H···O hydrogen bonds with non-planar geometry. Hydrogen bond distances are calculated 1.895 (CN-a), 1.898 (HN-a), 1.898 Å (DHN-a), for DFT method (B3LYP) and 1.872 (CN-a), 1.882 (HN-a), 1.858 Å (DHN-a), for M06–2X theory combined with 6-31G (*d*,*p*). The O–H hydrogen bond on dimer CN-a is indicated 1.87 Å in study of Sokolowska and Marciniak [32]. Binding abilities of hydrogen atom with hydroxyl oxygen on interactions are stronger at M06–2X theory than that of DFT method for all dimers. The differences are mainly ascribed to the existence of electro-

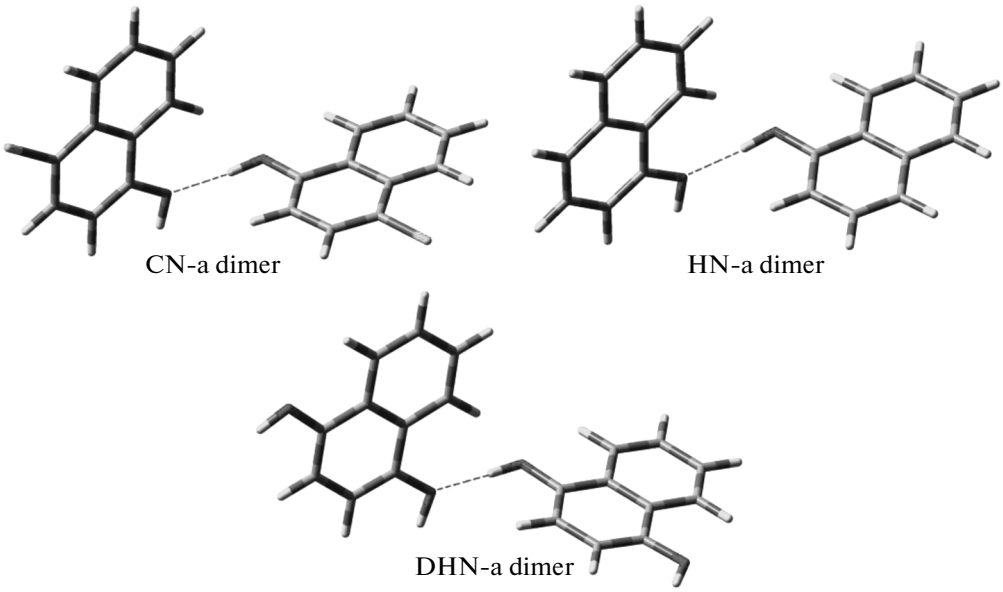

Fig. 4. Optimized dimer forms of CN, HN, and DHN at B3LYP/6-31G (*d*,*p*) basis set level.

static dipole-dipole interaction. Respectively, the calculated residual dipolc moments of CN-a, HN-a and DHN-a dimers formed with dipole-dipole interaction are higher values of 0.54, 0.02, and 0.06 D at M06–2X theory. The calculated binding energies with BSSE-corrected (uncorrected) values of the dimers are given in Table 6. BSSE-corrected binding energy differences at M06–2X calculations, more strongly bonds, are around 2.77, 2.71, and 2.82 kcal/mol for CN-a, HN-a, and DHN-a dimers with respect to B3LYP calculations, respectively, Intermolecular interactions between aromatic amino acid residues are studied by ab initio methods and binding energies are computed −5.8, −6.6 kcal/mol by second-order Møller-Plesset perturbation (MP2) theory and molecular mechanics (MM) simulations for *para*-cresol dimer labeled HB structures, respectively [36].

4. CONCLUSIONS

In this study, the most stable rotamers of CN, HN, and DHN compounds are determined by means of PES scans and relative energy calculations. The theoretical structural parametres, vibrational frequencies and NMR chemical shifts are obtained by using density functional theory method for these compounds on the ground stale forms. Generally, it can be said that the calculated results of the compounds were to be in a good agreement with the experimental data. This letter serves structurally stabilities and hydrogen bondings on CN-a, HN-a, and DHN-a dimers using DFT/B3LYP and M06 levels of calculations. Binding energies with BSSE-corrected/uncorrected values of the dimers arc higher at M06–2X functional than the other (B3LYP) calculations. These calculations aim to provide as a test of the efficacy of M06 calculations for intermolecular interactions and more strongly bound systems.

REFERENCES

1. J. E. Amoore and E. Hautala, J. Appl. Toxicol. **3**, 272 (1983).
2. J. P. Daw Son, W. W. Thayer and J. F. Desfoges, Blood **13**, 1113 (1987).
3. S. J. Fanbergh, Arch. Derm. Syph. **43**, 53 (1940).
4. M. Talukder and C. R. Kates, *Kirk-Othmer Encyclopedia of Chemical Technology* (Wiley, 1999-2014).
5. V. V. Mezheritskii, M. S. Korobov, O. M. Golyanskaya, N. I. Omelichkin, L. G. Minyaeva, G. S. Borodkin, A. A. Milov, A. V. Tsukanov, and A. D. Dubonosov, Russ. J. Org. Chem. **48**, 241 (2012).
6. M. I. Rodriguez-Caceres, R. A. Agbaria, and I. M. Warner, J. Fluoresc. **15**, 185 (2005).
7. P. D. Ahn, R. Bishop, D. C. Craig, and M. L. Scudder, J. Inclus. Phenom. Mol. Rec. Chem. **20**, 267 (1994).
8. P. D. Ahn, R. Bishop, D. C. Craig, and M. L. Scudder, J. Inclus. Phenom. Mol. Rec. Chem. **23**, 313 (1995).
9. Y. B. Rokade and R. Z. Sayyed, Rasayan J. Chem. **2**, 972 (2009).
10. A. Behal and B. Bahal, *A Textbook of Organic Chemistry* (S. Chand and Company, New Delhi, 2005).
11. B. P. Patel, E. J. Pressman, and R. Mills, Int. Patent WO/2005/040080 (2005).
12. S. Grimme, J. Comput. Chem. **27**, 1787 (2006).
13. J. Sponer, J. Leszczynski, and P. Hobza, J. Phys. Chem. **100**, 1965 (1996).
14. C. Lee, W. Yang, and R. G. Parr, Phys. Rev. B **37**, 78 (1988).

15. M. J. Frisch, G. W. Trucks, H. B. Schlegel, et al., *Gaussian 03,* Revision C.02 (Gaussian, Inc., Pittsburgh, PA, 2003).
16. D. C. Young, *Computional Chemistry: A Pratical Guide for Applying Techniques to Real-World Problems* (Wiley, New York, 2001).
17. M. H. Jamroz, *Vibrational Energy Distribution Analysis VEDA 4* (Warsaw, 2004).
18. A. Frisch, A. B. Nielsen, and A. J. Holder, *Gauss View User Manual* (Gaussian Inc., Pittsburgh, 2001).
19. R. Ditchfield, Mol. Phys. **27**, 789 (1974).
20. C. M. Rohlfing, L. C. Allen, and R. Ditchfield, Chem. Phys. **87**, 9 (1984).
21. S. Miertus, E. Scrocco, and J. Tomasi, J. Chem. Phys. **55**, 1171 (1981).
22. Y. Zhao and D. G. Truhlar, Theor. Chem. Acc. **120**, 215 (2008).
23. M. J. Frisch, G. W. Trucks, H. B. Schlegel, et al., *Gaussian 09*, Revision D.01 (Gaussian Inc., Wallingford CT, 2013).
24. S. F. Boys and F. Bernardi, Mol. Phys. **19**, 553 (1970).
25. R. Zhang, B. Du, G. Sun, and Y. Sun, Spectrochim. Acta, Part A **75**, 1115 (2010).
26. A. K. Jissy, U. P. M. Ashik, and A. Datta, J. Phys. Chem. C **115**, 12530 (2011).
27. E. Benassi and F. Spagnolo, J. Solution Chem. **39**, 11 (2010).
28. P. S. Liyanage, R. M. de Silva, and K. M. N. de Silva, J. Mol. Struct.: THEOCHEM **639**, 195 (2003).
29. M. C. R. Delgado, V. Hernandez, J. Casado, J. T. Lopez Navarre, J. M. Raimundo, P. Blanchard, and J. Roncali, J. Mol. Struct. **651**, 151 (2003).
30. J. P. Abraham, D. Sajan, V. Shettigar, S. M. Dharmaprakash, I. Nemec, I. H. Joe, and V. S. Jayakumar, J. Mol. Struct. **917**, 27 (2009).
31. M. Karabacak, M. Cinar, M. Kurt, A. Poiyamozhi, and N. Sundaraganesane, Spectrochim. Acta, Part A **117**, 234 (2014).
32. E. R. Sokolowska and B. Marciniak, Acta Crystallogr. C **65**, 207 (2009).
33. Sigma-Aldrich Electronic Web Page (Sigma Co., Aldrich, New York, 2006), http://www.sigmaaldrich.com/spectra/ftir/FTIR007548.PDF (Accessed March 2013); http://www.sigmaaldrich.com/spectra/rair/RAIR012403.PDF (Accessed March 2013).
34. B. Lu, L. Zeng, J. Xu, Z. Le, and H. Rao, Eur. Polym. J. **45**, 2279 (2009).
35. Spectral Database for Organic Compounds (National Institute of Advanced Industrial Science and Technology, Japan, 2011). http://sdbs.db.aist.go.jp (Accessed March 2013).
36. F. L. Gervasio, R. Chelli, P. Procacci, and V. Schettino, Proteins **48**, 117 (2002).